

Dynamic Vertex Replacement Grammars

Daniel Gonzalez Cedre

University of Notre Dame
Notre Dame, USA

Justus Isaiah Hibshman

University of Notre Dame
Notre Dame, USA

Timothy La Fond

Lawrence-Livermore Nat'l Lab.
Livermore, USA

Grant Boquet

Lawrence-Livermore Nat'l Lab.
Livermore, USA

Tim Weninger

University of Notre Dame
Notre Dame, USA

Abstract

Context-free graph grammars have shown a remarkable ability to model structures in real-world relational data. However, graph grammars lack the ability to capture time-changing phenomena since the left-to-right transitions of a production rule do not represent temporal change. In the present work, we describe dynamic vertex-replacement grammars (DyVeRG), which generalize vertex replacement grammars in the time domain by providing a formal framework for updating a learned graph grammar in accordance with modifications to its underlying data. We show that DyVeRG grammars can be learned from, and used to generate, real-world dynamic graphs faithfully while remaining human-interpretable. We also demonstrate their ability to forecast by computing divergence scores, a novel graph similarity measurement exposed by this framework.¹

1. Introduction

Like the string grammars upon which they are based, graph grammars usually deal with static data. Although it might be attractive to think of LHS \rightarrow RHS replacement schemes as indicative of change, growth, or evolution over time, this is rarely the case in grammar-based formalisms. Instead, grammars are typically used to represent hierarchical refinements of a static structure. The replacements that occur by applying production rules rarely have anything to do with time.

However, modeling time-varying data for real-life processes is fundamentally important for many scholars and scientists. Because graphs are capable of expressing immensely-complicated discrete topological relationships, they are widely used to model real world phenomena. In particular, temporal graph models have come to prominence

to account for the time-varying nature of many real phenomena. For example, the Temporal Exponential Random Graph Model (TERGM) [18], Dynamic Stochastic Block Model (ARSBM) [27], and certain versions of newer Graph Neural Network models (GraphRNN, GRAN) [26, 41] are able to fit sequential graph data and make predictions about future relationships, but these models are difficult to inspect and tend to break down.

Graph grammars have seen a recent increase in popularity, with applications in molecular synthesis [15, 23, 39], software engineering [24, 25], and robotics [43]. Related models focusing on subgraph-to-subgraph transitions are readily interpretable, but need to be hand-tuned to model subgraphs of a predetermined (usually very small) size, usually for computational complexity reasons [5, 20]. These transition models tend to set out a schema for the set of permitted transitions and perform modeling by simply counting transition frequencies. Despite their simplicity, these transition models are effective tools for understanding changes in dynamic systems. However, these models struggle with larger changes outside of 3-or-4-node (or similarly small) subgraph sizes [30].

More recently, researchers have found data-driven ways to learn representative hyperedge replacement grammars (HRG) [2, 38] and vertex replacement grammars (VRG) [32, 33]. These models permit the extraction of production rules from a graph and the resulting grammar can be used to reconstruct the graph or generate similar graphs. However, as discussed earlier, these models are still limited by the inherent static nature of the formalism. The lack of a dynamic, interpretable, learnable model presents a clear challenge to modeling real-world relational data.

In the present work, we tackle this challenge by introducing the **Dynamic Vertex Replacement Grammars** (DyVeRG). As the name implies, this model extends the VRG framework, which typically begins with a hierarchical clustering of the graph and then extracts graph rules in a

¹<https://github.com/daniel-gonzalez-cedre/DyVeRG>.

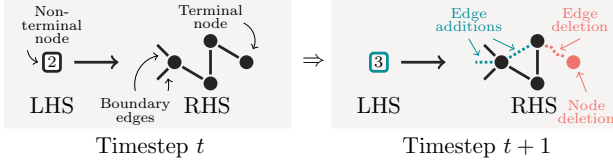


Figure 1. An example of a rule transition comprised of two production rules: the left-rule extracted from a graph at time t and the right-rule updated at time $t + 1$. Here we see evidence of triadic closure, the disappearance of a node with its incident edge, and resulting changes to the LHS symbol.

bottom-up fashion from the resulting dendrogram. In order to adapt VRGs to the dynamic setting, the DyVeRG model finds stable mappings between filtrations of the nodes in the dynamic graph across time. The filtration mappings provide a transparent way to inspect the changes in the graph without significant performance degradation.

This dynamic graph grammar takes the form of a sequence of production rules we call *rule transitions* that are interpretable and inspectable. An example of such a rule transition is illustrated in Fig. 1: the rule on the left is extracted from a graph G_t at time t ; the rule on the right covers the same nodes, but corresponds to time $t + 1$ and incorporates changes from G_{t+1} . In this example, the nonterminal node on the LHS of the left production rule signifies that the RHS has two boundary edges (used to connect elsewhere in the graph). The RHS also has four terminal nodes and three terminal edges. However, as the graph changes between times t and $t + 1$, the topology of the rule on the right of Fig. 1 changes correspondingly. The blue dotted edges illustrate the addition of one terminal edge and one new boundary edge, which is why the nonterminal label on the LHS increased from 2 to 3. The red nodes and wavy dotted lines represent the deletion of a node and edge respectively across this temporal chasm.

The paper is organized as follows. We first introduce some basic concepts and terminology. Then, we describe the DyVeRG model with the help of illustrations and examples. We then introduce the divergence score, a byproduct of DyVeRG, and explain how rudimentary forecasting can be done as well as the more-traditional graph generation. Finally, we provide a quantitative and qualitative analysis of the model on real-world dynamic graphs and compare its predictive performance against other generative models.

2. Preliminaries

A graph $G = (V, E)$ is a set of nodes V with a relation $E \subseteq V \times V$ defining edges between the nodes. We say that G is connected if there is a path within G between any two nodes. If E is symmetric, then we say G is undirected; otherwise, G is directed. We say that G is node-labeled if

we have a function $\lambda : V \rightarrow L$ that assigns a label from L to each node in G . If we have two such node-labeling functions, we call the graph doubly-node-labeled. We say that G is edge-weighted if we have a function $\omega : E \rightarrow W$ assigning each edge in the graph some weight from W . If these weights are natural numbers, then we say G is a multigraph, whose edge multiplicities are given by ω .

There are two common ways to model temporality for graphs: as continuous streams of (hyper-)edges, and as discrete sequences of graph snapshots [22]. In the present work, we consider the latter form of dynamic graph, which we represent as a (finite) sequence $\langle G_t \rangle_{t=0}^T = \langle G_0, \dots, G_T \rangle$ of graphs $G_t = (V_t, E_t)$.

2.1. Context-Free Grammars.

A context-free grammar (CFG) on strings is determined by a finite set of nonterminal symbols N with a distinguished starting symbol $S \in N$ and finite a set of terminal symbols T , along with a finite set of production rules $R \subseteq N \times (N \cup T)^*$. Each rule $P_i \in R$ represents a transition from a left-hand side (LHS) nonterminal to a finite sequence of symbols on the right-hand side (RHS), each of which is either terminal or nonterminal. We say P_i is terminal if it only contains terminal symbols; otherwise, P_i is nonterminal.

Given a string $\Sigma = \sigma_1 \dots \sigma_i \dots \sigma_n \in (N \cup T)^*$, the application of a production rule P_i to a particular nonterminal symbol $\sigma_i \in N$ from Σ involves replacing the symbol σ_i with the string on the RHS of P_i . Formally, the result of applying $P_i = (\sigma_i, \pi_{P_i})$ to σ_i in Σ is a new string $\tilde{\Sigma} = (\sigma_1 \dots \sigma_{i-1}) \cdot \pi_{P_i} \cdot (\sigma_{i+1} \dots \sigma_n)$, where \cdot represents the string-concatenation operation.

2.2. Vertex-Replacement Graph Grammars.

A natural way to generalize CFGs would be to think of the characters in a string like nodes in a graph. We can then think of CFG rules as producing graphs whose nodes are arranged in a path, with attributes given by the different characters in the language and boundary conditions specifying whether or not additional characters can be added at the beginning or end of the string. Clearly, changing the connectivity structure and boundary conditions will lead to rules with more expressive RHS structures.

There are many specific formalisms and nuances, but generally a vertex-replacement grammar (VRG) is given by a finite set of nonterminal symbols $N \subseteq \mathbb{N}$ with the distinguished starting symbol $0 \in N$ along with a set of terminal symbols $T \subseteq V_G$ representing nodes in a graph. The production rules P_i for a VRG then look like transitions from a nonterminal symbol $n \in N$ to a doubly-node-labeled multigraph (H, λ_H, δ_H) whose first node-labeling function $\lambda_H : V_H \rightarrow N \cup T$ distinguishes between terminal and nonterminal symbols, and whose second node-labeling

function $\delta_H : V_H \rightarrow \mathbb{N}$ assigns a natural number *boundary degree* to each node of G .

As was the case with CFGs, we apply rules at nonterminals by replacing those symbols with the structure on the RHS of a suitable production rule, while accounting for VRG rules’ nontrivial boundary conditions (*i.e.*, the boundary degrees). Given a connected, node-labeled multigraph $G = (V_G, E_G, \lambda_G)$ with a node $v \in V_G$ having nonterminal label $\lambda_G(v) \in N$, the application of a rule $P_i = (\lambda_G(v), (H, \lambda_H, \delta_H))$ at v consists of replacing v with the graph H and rewiring the *broken edges*—those edges previously connected to v —to those nodes in H such that the number of broken edges incident on a node v_H of H does not exceed its boundary degree $\delta(v_H)$.

Random rewiring is the most rudimentary way to address the boundary condition. If our data were augmented with node labels, we could guide the rewiring process using an estimated assortativity mixing matrix, or by minimizing a loss function computed over the nodes [33]. Even without node labels, we could consider greedy rewiring strategies that try to reduce discrepancy along some measured statistic of the data—*e.g.*, modularity, average local clustering coefficient, graphlet distribution. For simplicity, we consider only the random approach in the present work.

Formally, we will say that a production rule $P_i = (s, (H, \lambda_H, \delta_H))$ is suitable for a node $v \in V_G$ if $\lambda_G(v) = s$ and $\deg(v) = \sum_{v_H \in V_H} \delta_H(v_H)$. This means that the label associated with v is the same as the nonterminal symbol P_i is expecting, and that the number of broken edges v will leave behind is the same as the total number of boundary edge slots H has available. With these conditions, the application of a suitable P_i at a node v results in a well-defined, though not necessarily deterministic, vertex-to-subgraph substitution.

Typically, we only distinguish between the rules in a grammar *up to isomorphism* once an appropriate notion of isomorphism for production rules is specified. We say two rules $\dot{P} = (\dot{s}, (\dot{H}, \dot{\lambda}, \dot{\delta}))$ and $\ddot{P} = (\ddot{s}, (\ddot{H}, \ddot{\lambda}, \ddot{\delta}))$ from a VRG are rule-isomorphic *if and only if* $\dot{s} = \ddot{s}$ and there is a graph isomorphism $\dot{H} \cong \ddot{H}$ that preserves the labels from $\dot{\lambda}$ and $\ddot{\lambda}$ (but not necessarily $\dot{\delta}$ and $\ddot{\delta}$).

2.3. Filtrations.

A filtration of a graph $G = (V, E)$ is a sequence of node partitions $\mathcal{F} = \langle F_i \rangle_{i=1}^n$, where each F_i partitions the node set V into mutually-disjoint subsets—called *covers*—so that each F_i is a refinement of F_{i+1} . When mining real-world networks, filtrations are often the result of hierarchical node clusterings [4, 13], k -core decompositions [11, 31], and, more recently, methods [28, 34] inspired by persistent homology [10] and topological data analysis [7]. The aforementioned methods usually produce filtrations as an intermediate result for an analysis of a network involving, for

example, community detection [42], representation learning [40], or visualization [9]. Filtrations lend themselves well to generative approaches to network structures since they can highlight salient hierarchical and recursive patterns. Vertex-replacement graph grammars can induce filtrations (*cf.* Sec. 3.1) suitable for dynamic graph modeling.

3. Dynamic Vertex-Replacement Grammars

Incredible advances in theory and application have enabled researchers to parse real-world networks by learning an appropriate graph grammar—including vertex replacement schemes [15, 32, 33], hyperedge replacement schemes [2, 38], and Kemp-Tennenbaum [19] grammars. An important limitation of these established formalisms is their semantic inability to express temporality in terms of change to their underlying data. This presents a serious problem for practitioners: time does not stand still, and new data may lead to changes in prior beliefs. By associating the grammar extracted from a dataset with a filtration on the data, and describing how filtrations on graphs produce compatible grammars, we construct temporal transitions between grammars by defining transitions between their associated filtrations, which are driven by changes in the data. In the proceeding sections, we detail the **Dynamic Vertex-Replacement Grammar (DyVeRG)** framework for generalizing VRGs in the time domain.

3.1. Extracting Rules.

We describe in this section how to parse a graph with a VRG and how its associated filtration is computed. For simplicity, we focus on just two temporally-sequential graphs $G_t = (V_t, E_t)$ and $G_{t+1} = (V_{t+1}, E_{t+1})$ at a time, though the idea generalizes to an arbitrarily-long finite sequence of graphs. First, an initial filtration $\mathcal{F}_t^{\text{clust}}$ on G_t is produced using the Leiden hierarchical clustering algorithm [35]. We choose to use Leiden for our analyses as opposed to the myriad alternatives—the Louvain algorithm [6], smart local moving [36], hierarchical Markov clustering [37], recursive spectral bi-partitioning [17]—because its iterative modularity-maximization approach is intuitively appealing, and it realizes better performance [35] than Louvain and smart local mover (on which Leiden is based) while remaining efficient on larger graphs.

Taking inspiration from clustering-based node replacement grammars [32], we use the filtration $\mathcal{F}_t^{\text{clust}}$ derived from the hierarchical clustering to recursively extract rules for the grammar. Starting from the bottom, we consider subfiltrations covering at most μ nodes (terminal or nonterminal) total, where $\mu \in \mathbb{N}_+$ is set *a priori* to limit the maximum size of any rule’s RHS. Among all subfiltrations of size at-most μ , we then select a subfiltration \mathcal{F}^* that minimizes the overall description length of the grammar. \mathcal{F}^* then determines a rule P^* that gets added to our grammar

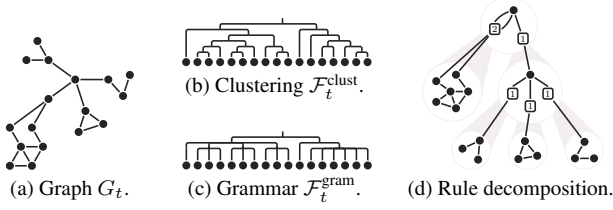


Figure 2. Overview of the extraction process for a VRG on a static graph G_t pictured in (a). A filtration induced by a hierarchical clustering is shown in (b), from which the rules in (d) are extracted bottom-up. At the same time, the filtration in (c) is derived from the node coverings the extracted rules produce.

and $\mathcal{F}_t^{\text{clust}}$ is compressed until every node is in the same cover, as described by Sikdar *et al.* [32].

Concurrently, we also construct a filtration $\mathcal{F}_t^{\text{gram}}$ whose node covers are determined by the right-hand sides of the rules in the grammar as they are extracted. The filtration $\mathcal{F}_t^{\text{gram}}$ acts as a rule-based hierarchical decomposition of G_t , keeping track of the parallel hierarchical structure shared by the rules in the grammar and the nodes in the graph. This naturally produces a one-to-one correspondence between the rules $R_t = \{P_{t,1}, \dots, P_{t,r}\}$ in our (unweighted) grammar and their corresponding covers in $\mathcal{F}_t^{\text{gram}}$, allowing us to construct a surjective association $f_t : V_t \rightarrow R_t$ between each node $v \in V_t$ and the unique rule $f_t(v) \in R_t$ that was extracted with v as a terminal node. Further, we keep track of the particular terminal symbol node on the right-hand side of $f_t(v)$ corresponding to v when $f_t(v)$ was extracted. We call this $\alpha_t(v)$, the *alias* of v , where $\alpha_t : V_t \hookrightarrow T$. An illustration of this process on a small example network is shown in Fig. 2. The two filtrations are highlighted along with a hierarchical decomposition of the graph induced by the grammar’s rules.

The *root* of a grammar is defined to be the rule whose left-hand side is the distinguished starting symbol S . Clearly, this rule covers every node in G_t . Given two rules $\dot{P}_t, \ddot{P}_t \in R_t$, we say \dot{P}_t is an *ancestor* of \ddot{P}_t iff every node covered by \ddot{P}_t in the filtration is also covered by \dot{P}_t . If additionally $\dot{P}_t \neq \ddot{P}_t$, then it is a *proper ancestor*. We define one rule to be a *descendant* of another conversely to how ancestors are defined. Finally, a *common ancestor* of a set of rules $\tilde{R}_t \subseteq R_t$ is rule \hat{P}_t that is an ancestor of rule in \tilde{R}_t , and the *least common ancestor* is the one having no common ancestor of \tilde{R} as a proper descendant. Note that the least common ancestor of a nonempty subset of R_t always exists since the root rule is an ancestor of every rule in \mathcal{G}_t .

3.2. Updating the Filtration

We will refer interchangeably to the covers in the filtration $\mathcal{F}_t^{\text{gram}}$ and the rules $P_{t,i} \in R_t$ in the grammar \mathcal{G}_t . For a visual summary of the preceding description, please refer

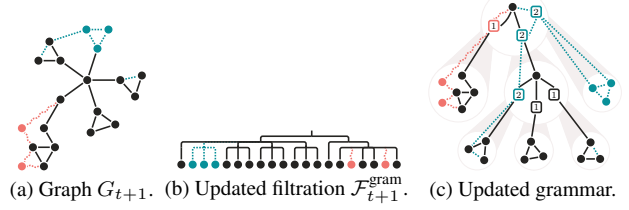


Figure 3. The graph from Fig. 2a, the filtration from Fig. 2c, and the grammar from Fig. 2d are shown here with changes from time t to $t+1$. The changes to G_{t+1} in (a) stimulate changes to the filtration in (b), modifying the corresponding rules in the grammar (c). Following Fig. 1, the node and edge addition is shown in blue, while node and edge removal is indicated in red. Nonterminal nodes’ borders are colored blue or red if they increased or decreased in value respectively.

to Fig. 3. First, we categorize the edges $(u, v) \in E_t \cup E_{t+1}$:

- I. *persistent*: $u \in V_t, v \in V_t, u \in V_{t+1}, v \in V_{t+1}$, and $(u, v) \in E_t \cap E_{t+1}$
- II. *internal additions*: $u \in V_t, v \in V_t, u \in V_{t+1}, v \in V_{t+1}$, and $(u, v) \in E_{t+1} \setminus E_t$
- III. *frontier additions*: $u \in V_t, v \notin V_t, u \in V_{t+1}, v \in V_{t+1}$, and $(u, v) \in E_{t+1} \setminus E_t$
- IV. *external additions*: $u \notin V_t, v \notin V_t, u \in V_{t+1}, v \in V_{t+1}$, and $(u, v) \in E_{t+1} \setminus E_t$
- v. *edge deletions*: $u \in V_t, v \in V_t$, and $(u, v) \in E_t \setminus E_{t+1}$

Examples of edges from each category are demonstrated in Fig. 4. These classes determine how each edge induces a change in the filtration: class I. edges do not influence the filtration, class II. edges add new connections between already-existing nodes (thus altering the induced subgraph covers of the filtration) class III. edges introduce a new neighbor for an already-existing node, class IV. edges produce two entirely-new neighboring nodes, and class v. edges account for the removal of connections from the graph, which may or may not be associated with nodes’ exodus from the network. Of these, only classes III., IV., and v. are capable of causing structural changes to the hierarchy of the filtration, but all except for class I. edges will affect the grammar’s rules.

3.2.1 Internal Additions.

If an edge (u, v) corresponds to an *internal addition*, we first find the covering rules $f_t(u) = P_u$ and $f_t(v) = P_v$ of the nodes incident on that edge and let G_u and G_v be their respective RHS graphs. If $G_u = G_v$, then we simply add an edge between $\alpha_t(u)$ and $\alpha_t(v)$. However, if $G_u \neq G_v$, then we find their least common ancestor and add an

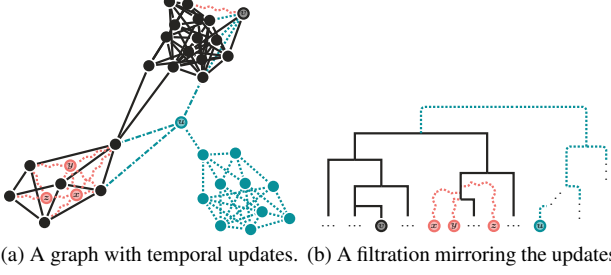


Figure 4. A dynamic graph with three well-defined communities (a) and an associated filtration (b) are shown with temporal updates. Class I. edges are shown in solid black. The blue dotted edges incident to v in (a) are class II. edges; the blue dotted edges between u and the black nodes are class III. edges; all other blue dotted edges are class IV. edges. The wavy edges in red belong to class V.

edge between the appropriate nodes on its right-hand side. Note that if a nonterminal symbol is incident on the edge added, then this will necessarily change the symbol—recall that the nonterminal symbols are defined to be the sum of their degree with their boundary degree. This change in the symbol must be propagated *down* through the hierarchy by commensurately increasing LHS’s of rules and adding boundary degrees.

3.2.2 Frontier & External Additions.

We handle frontier and external edge additions jointly by cases. Given an edge (u, v) of class III. or IV., let $H_{(u,v)} \triangleleft G_{t+1}$ be the maximally connected induced subgraph of G_{t+1} containing (u, v) .

In the first case, suppose none of the vertices of $H_{(u,v)}$ coincide with G_t . We begin by independently extracting a grammar $\mathcal{H}_{(u,v)}$ on $H_{(u,v)}$ with its own induced filtration. We then *merge* this grammar with \mathcal{G}_t by combining the two filtrations under one larger cover. Specifically, this takes the form of a new root rule whose LHS is S and RHS consists of two disconnected nonterminal symbols—one for G_t and one for $H_{(u,v)}$ —incorporating the rules of \mathcal{G}_t and $\mathcal{H}_{(u,v)}$ as descendants. To disambiguate, the LHS’s for the root rules \mathcal{G}_t and $\mathcal{H}_{(u,v)}$ are updated accordingly.

In the second case, there is at least one node in common between $H_{(u,v)}$ and G_t . Define the *frontier* $F(G_t, H_{(u,v)})$ between G_t and $H_{(u,v)}$ to be the collection of all such class III. edges. Then, for each edge $(u_G, v_H) \in F(G_t, H_{(u,v)})$, we find the rules $f_t(u_G) = P_{u_G}$ and P_{v_H} from \mathcal{G}_t and $\mathcal{H}_{(u,v)}$ that cover u_G and v_H respectively, and increase their boundary degrees by 1 to indicate that this node should expect to receive a new edge. This increase in boundary degree necessitates a change to the LHS symbols of the two rules, which in turn induces more changes to their ancestor rules; these changes propagate *up* to the roots of their re-

spective hierarchies. Finally, once these changes have been made for each frontier edge, a new rule is created (*cf.* the prior case) with two nonterminal symbols connected by as many edges as there are in $F(G_t, H_{(u,v)})$, concluding the subgrammar-merging process. This accounts for all of the class III. and IV. edges that participated in the connected component $H_{(u,v)}$.

3.2.3 Deletions.

An edge deletion (u, v) must have both of its incident nodes existing in G_t , but they need not exist in G_{t+1} . As a result, we handle class V. edges by first finding the covering rules $f_t(u)$ and $f_t(v)$ and removing the edge between the nodes corresponding to $\alpha_t(u)$ and $\alpha_t(v)$ from their common ancestor. Note that if this edge was incident on a nonterminal symbol, its removal will cause a cascade of changes that must be propagated *down* the hierarchy. Then, if u is not present in G_{t+1} , we also remove the node $\alpha_t(u)$ from the RHS of $f_t(u)$; similarly with v and the removal of $\alpha_t(v)$ from $f_t(v)$.

3.3. Measuring Deviation

Now that we know how to take a grammar \mathcal{G}_t and temporally modify it into \mathcal{G}_{t+1} , we can analyze what the specific changes were between the two grammars. From the process delineated in Sec. 3.1, we obtain a natural correspondence $\pi_t : R_t \rightarrow R_{t+1}$ between every rule $P_t \in R_t$ from \mathcal{G}_t and its updated version $\pi_t(P_t) \in R_{t+1}$ in \mathcal{G}_{t+1} . We can use this mapping to quantify the difference between the two grammars in terms of the number of changes introduced by the temporal update process. Given a rule $P_{t+1} \in R_{t+1}$, we define the change introduced by this rule by computing the graph edit distance (GED) [1] between the RHS’s of P_{t+1} and $\pi_t^{-1}(\{P_{t+1}\})$ (with a small penalty to any modifications that need to be made to make the LHS’s the same)². If P_{t+1} is a rule introduced as part of the subgrammar-merging process for class III. and IV. edges, then we let $\pi_t^{-1}(\{P_{t+1}\})$ be the empty graph by definition. By aggregating these edit distances across the rules of \mathcal{G}_{t+1} , we get an indication of how much \mathcal{G}_t had to be perturbed to accommodate the data seen in G_{t+1} . Specifically, we compute

$$\Delta = -\ln \frac{1}{1 + \sum_{P_{t+1} \in R_{t+1}} \text{GED}(\pi_t^{-1}(\{P_{t+1}\}), P_{t+1})}. \quad (1)$$

3.4. Generating Graphs

Finally, we can use the rules from the updated grammar \mathcal{G}_{t+1} to generate graphs. First, we post-process the rules of the unweighted grammar \mathcal{G}_{t+1} into the rules of a weighted grammar by combining all isomorphic rules and weighting

²The notation $\pi_t^{-1}(\{P_{t+1}\})$ denotes the *preimage* of P_{t+1} under π_t .

Table 1. Summary of the datasets used in the evaluation.

	node count	edge count	# timestamps	# interactions	# snapshots
DNC Emails	1 891	4 465	19 389	32 878	11
EU Emails	986	16 064	207 880	327 333	19
DBLP	95 391	164 479	21	200 792	21
Facebook	61 096	614 797	736 674	788 135	29

them by how frequently (up to isomorphism) each rule occurred in \mathcal{G}_{t+1} . The idea now is identical to the approach traditionally taken by weighted VRGs. We start with the root rule, which has LHS symbol S , and use the structure on its RHS as our initial graph \hat{G}_{t+1} . We then iteratively grow the graph by randomly selecting a nonterminal symbol in \hat{G}_{t+1} and randomly sampling a compatible rule to apply at that symbol, with the sampling probability for the rules determined by the frequencies of the possible candidate rules for that nonterminal symbol. Once no nonterminal symbols remain in \hat{G}_{t+1} , we stop and obtain our resulting graph.

4. Evaluation

We perform three types of analysis to better understand the quantitative and qualitative characteristics of the DyVeRG model. In the first quantitative benchmark, we task the model with distinguishing genuine temporal dynamics from realistic imposter data created by other generative models. The second quantitative analysis asks all of the models, including DyVeRG, to generate a graph corresponding to a slice of time from the data; the generated graphs are then compared to the ground truth. We conclude with a short qualitative analysis and interpretation of the temporal transitions DyVeRG induces between grammar rules.

4.1. Datasets

In this evaluation, we consider four dynamic datasets, listed in Tab. 1. DNC Emails and EU Emails are email networks where user email accounts are nodes and an email from one user to another at a given time is represented by an undirected edge labeled with a UNIX time. Both of these datasets are aggregated by month; DNC Emails contains a number of self-edge loops, while EU Emails contains none. The DBLP dataset is an undirected academic coauthorship graph where nodes correspond to researchers and an edge is drawn between two researchers during a particular year *iff* they coauthor a paper during that year. Finally, the Facebook dataset is an undirected graph tracking friendships on a monthly basis, with two users sharing an edge if they were friends during that month.

We take snapshots 0 through 10 for each dataset. Because these datasets are dynamic, we summarize their orders and sizes in Fig. 5, noting they tend to grow over time.

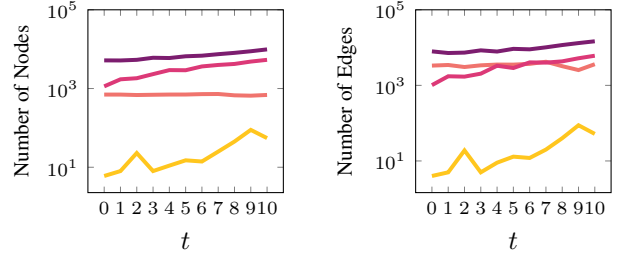


Figure 5. Number of nodes and edges in the datasets over time.

4.2. Baselines

We compare the DyVeRG model against 5 baselines. The Erdős-Renyi model generates random graphs of a fixed size n with probability p of an edge between any two nodes [12]; for evaluation we set n and $p = 2^m/n(n-1)$ to the ground-truth values within each timestep. The configuration model of Chung and Lu generates a random graph approximating a given degree distribution [8, 16]; for this baseline, we use the degree distribution from the dataset.

The Erdős-Renyi and Configuration models learn very rudimentary features from an input graph. The following three graph models are different in that they take a whole graph as input and use their own inductive biases to learn features. The Stochastic Block Model (SBM) uses matrix reductions to represent graphs with structured communities [21, 29]. Likewise, the more advanced graph recurrent neural network (GraphRNN) [41] is able to learn a generative model from an input collection of graphs by adapting walks over nodes as sequential data. We also provide a static implementation of DyVeRG based on CNRG [32], which we call VeRG, as a final point of comparison.

An important note should be made here that some of the data for GraphRNN is missing from the figures. This is because, when training and testing the model on the two NVIDIA GeForce RTX 2080 Ti cards available to us, with 10 GB of RAM each, we regularly ran out of memory on the larger datasets.

4.3. Inference

The goal of this task, given a temporal sequence of graphs $\langle G_t \rangle_{t=0}^{10}$, is to distinguish the graph that genuinely comes next from an assortment of impostors.

For each timestep $t \in \{0, \dots, 9\}$, we extract a VRG from G_t and update it using G_{t+1} , yielding DyVeRG grammars $\langle \mathcal{G}_t \rangle_{t=1}^{10}$. These grammars are used to compute dyvergence scores (cf. Sec. 3.3) for the ground truth. This is performed 10 times independently for each (G_t, G_{t+1}) pair, and we let D_t denote the mean.

We use the average ground-truth dyvergences

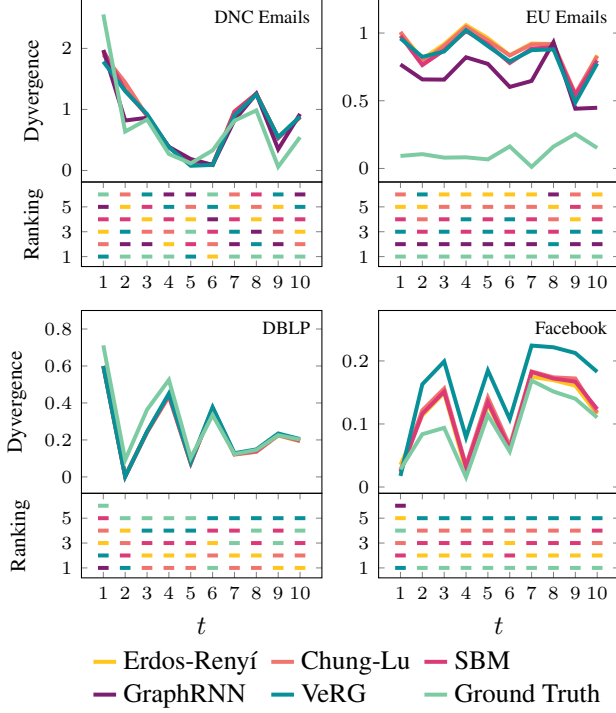


Figure 6. Dyvergence scores and model rankings. The top subplots show, for each model, the deviations over time from the mean dyvergence score. The relative rankings of the models are then shown in the corresponding bottom subplots. Note that lower is better, so the best-performing model is listed at the bottom.

$\{D_0, \dots, D_{t-1}\}$ to compute an estimate \hat{D}_t for the expected dyvergence of the next graph pair (G_t, G_{t+1}) —*i.e.*, an estimate for D_t . Specifically, we let $A_t = (\sum_{i=0}^t D_i)/(t+1)$ and compute

$$\hat{D}_t = A_{t-1} + (D_{t-1} - A_{t-2}). \quad (2)$$

Separately, each impostor model \mathcal{M} is trained on G_{t+1} and 10 graphs $\langle M_{t+1,i} \rangle_{i=1}^{10}$ are sampled from its distribution. Dyvergence scores are calculated for these graphs by extracting a VRG from G_t and then updating it with each of the $M_{t+1,i}$; aggregate edits are then computed as in Eq. 1. Average dyverages $D_{\mathcal{M},t}$ are then found for the $(G_t, M_{t+1,i})$. We define the *dyvergence* of \mathcal{M}_t by

$$\text{dyvergence}(G_t, \mathcal{M}_t = |\hat{D}_t - D_{\mathcal{M},t}| \quad (3)$$

Dyvergence for the ground truth is similarly defined by $\text{dyvergence}(G_t, G_{t+1}) = |\hat{D}_t - D_t|$. The lower this score is, the higher our confidence would be that the scored graph comes from the same generating distribution as the data.

We illustrate our results in Fig. 6. Here, we determine success by assigning the ground truth a lower dyvergence score than the impostor graphs. We outperform the competing baselines on the EU Emails and Facebook datasets.

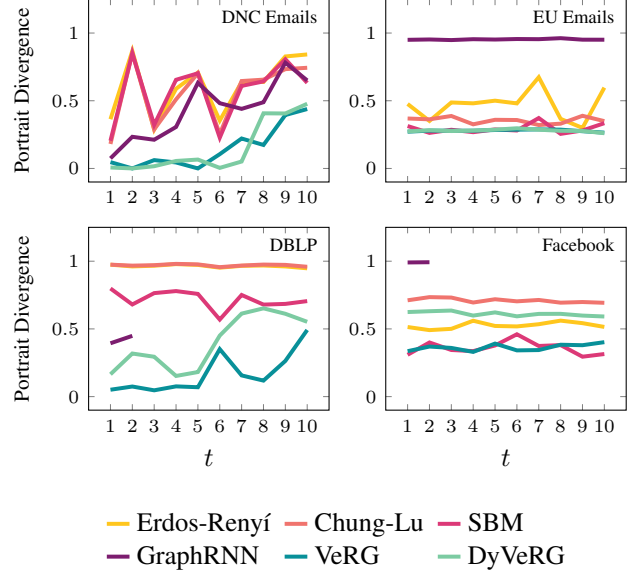


Figure 7. Portrait Divergence comparing a generated graph from each model and timestep against a corresponding ground truth graph. Lower is better.

Our model is also largely successful on the DNC email graph, ranking the ground truth as least-dyvergent the majority of the time, shown clearly by the ranking subfigures in Fig. 6. The model performs poorly only on the DBLP graph. We conjecture that the amount of dyvergence in DBLP from one time step to another fluctuates more drastically due to the longer timescale for data aggregation in this dataset; whereas the other three datasets were grouped into monthly snapshots, DBLP snapshots are taken annually. This might lead to inaccuracies in \hat{D}_t , negatively impacting the dyvergence scores for the real graph while boosting performance on imposters that are not as temporally turbulent.

4.4. Generation

A natural way to interrogate a generative graph model—like a graph grammar—is to generate graphs with it. Generative graph models are widely used in modern AI systems for contrastive and adversarial learning. Here, we use these models in the more traditional way they might be used for a task like hypothesis-testing; we fit the models, generate a graph at a particular time, and then compare the generated graph with the ground truth. For each baseline model, we train on the ground truth at time t and then generate at this same time. If the two graphs are similar according to some empirical measure of graph similarity, then we would say that the model performed well. For DyVeRG, we train on time $t-1$, update with time t , and then generate at time t .

Comparing two (or more) graphs is a nontrivial task since the distributions from which graphs can be sampled can behave erratically and are often very high-dimensional.

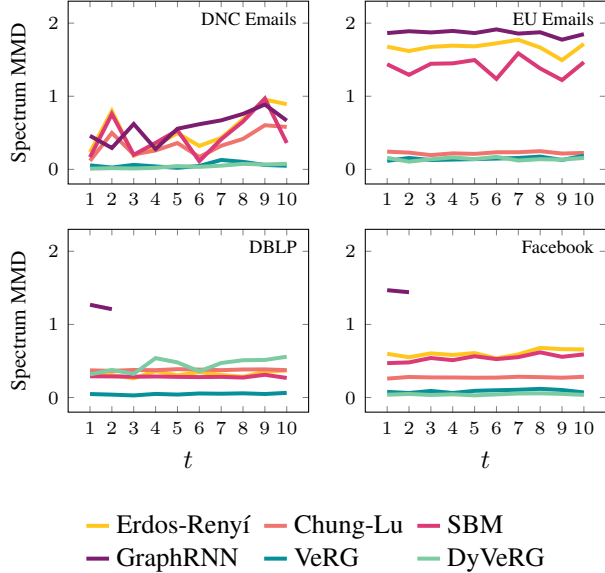


Figure 8. The MMD of the eigenvalues (Spectrum) of a generated graph from each model and timestep compared a corresponding ground truth graph. Lower is better.

The most natural way to determine similarity between two graphs is by an isomorphism test; however, in addition to being computationally intractable, this provides a far-too-narrow view of graph similarity. We instead take two alternative views to graph similarity. Graph portrait divergence [3] provides a holistic view of a graph based on a matrix of random-walk counts sorted by length; these results will be averaged across 10 independent trials. Maximum mean discrepancy (MMD) [14] is a kernel-based sampling test—which will thus not require any averaging—with desirable stability and computational efficiency characteristics. For both of these, lower is better.

We begin with the Portrait Divergence results, shown in Fig. 7. In general, we can see that the DyVeRG-generated graphs tend to have lower portrait divergence compared to the other models, thus outperforming them.

Next, we analyse the MMD of the eigenvalue spectra of the graphs’ Laplacian matrices. MMD values are bounded between 0 and 2, with a value of 0 indicating belief that the spectrum of the ground truth and the sample spectra of the generated graphs were certainly sampled from the same underlying distribution. These results are shown in Fig. 8. Here, we find that DyVeRG performs no worse than VeRG, its static counterpart, on three of the datasets. However, on the DBLP dataset, DyVeRG performs worse than almost all of the other models, despite its static analogue VeRG outperforming every model.

There are, of course, many additional metrics by which to compare these models, but the main power of DyVeRG comes from its ability to express graph dynamics in a

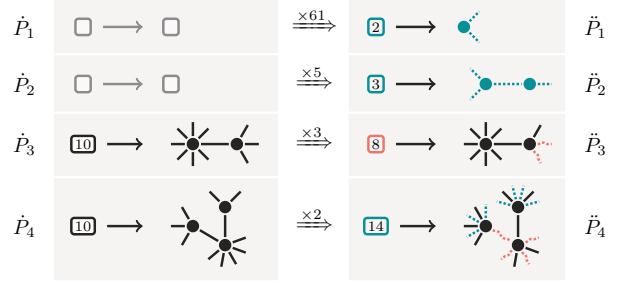


Figure 9. A sample of the top rule transitions from the EU Emails dataset. $\times 61$ denotes that the first rule transition was repeated 61 times. These rule transitions describe various changes in graph structure over time.

human-interpretable way.

4.5. Interpretability

To illustrate how the DyVeRG model can help a practitioner understand a complex temporal dataset, we illustrate some specific examples of frequent *rule transitions*—analogous to subgraph-to-subgraph transitions—learned by the model.

We focus our analysis here on the first 10 timesteps of the EU Emails dataset. For each $t \in \{0, \dots, 9\}$, we extract a grammar on G_t and then update it according to the procedure described in Section 3, giving us a list of DyVeRG grammars $\langle \mathcal{G}_t \rangle_{t=1}^{10}$. Then, given two rules \dot{P} and \ddot{P} , each of which could be a rule from any of the grammars \mathcal{G}_t for $t \in \{1, \dots, 10\}$, we say that a transition of type $\dot{P} \Rightarrow \ddot{P}$ has occurred *iff* there is a grammar \mathcal{G}_i such that, during the temporal updating procedure, a rule isomorphic to \dot{P} was modified into a rule isomorphic to \ddot{P} . We then go through our list of grammars and tally up the frequency with which every possible rule transition occurs with the idea in mind that the most frequent rule transitions might provide some salient insight into the dynamics of the dataset. In Fig. 9, we have a sample of four of the most frequent rule transitions learned from EU Emails, which we will refer to as $\dot{P}_1 \Rightarrow \ddot{P}_1, \dots, \dot{P}_4 \Rightarrow \ddot{P}_4$ respectively.

Both $\dot{P}_1 \Rightarrow \ddot{P}_1$ and $\dot{P}_2 \Rightarrow \ddot{P}_2$ illustrate that a new structure emerged at time $t + 1$ among nodes that did not already exist in G_t . In the first case, we have the introduction of a new user participating in a email exchange with two other people, and this occurs 61 times throughout the whole dataset. In the second, we can see a pair of new users emailing each other, one of whom has sent two emails elsewhere in the network and the other of whom has sent out one additional email, a structure that occurs 5 times in the data. In either case, because there was no rule at time t that \dot{P}_1 and \dot{P}_2 are updated versions of, we can be certain they were additions that participated in a larger connected component that was introduced wholly at time $t + 1$. This

reveals a temporal property of the EU Email network: it is much more frequent for users to send out emails following periods of inactivity when other previously-inactive users are also sending out emails to new people, than it would be for them to suddenly begin sending emails to active users.

The next transition, $\dot{P}_3 \Rightarrow \ddot{P}_3$, shows us that three times throughout the data, a heterophilous dyad—a communicating pair of users where one is involved in many emails and the other is not—will see a reduction in the number of emails in which the less popular user participates. By contrast, the final transition $\dot{P}_4 \Rightarrow \ddot{P}_4$ exemplifies a more extreme version of the *opposite* phenomenon: twice in the data, when a heterophilous wedge consisting of two unpopular users is bridged by a high-volume email-sender, the bridging user will experience a reduction in email output while the unpopular users become more popular.

The insights obtained by this analysis are over-specific due largely to the precise nature of rule isomorphism. However, if a more relaxed view of rule isomorphism is adopted, and the definition of rule transition is broadened, then our model could describe even more general temporal trends. Even so, our model has shown its ability to provide significant insight into network dynamics.

5. Conclusion

We introduced the **Dynamic Vertex Replacement Grammar (DyVeRG)** formalism, which is a graph grammar model that learns rule transitions from a dynamic graph. Unlike typical graph grammars, these rule transitions encode the dynamics of a graph’s evolution over time. Further, unlike subgraph-to-subgraph transition models, which learn transitions between small configurations of nodes, DyVeRG encodes rule transitions across multiple levels of granularity.

We show through our quantitative analysis across two tasks and three metrics that the fidelity of the DyVeRG model is comparable or better than many existing graph models, even a highly-parameterized, uninterpretable graph neural network. Finally, we presented a short case study demonstrating how the induced rule transitions can provide insight into a temporal dataset.

References

- [1] Zeina Abu-Aisheh., Romain Raveaux., Jean-Yves Ramel., and Patrick Martineau. An exact graph edit distance algorithm for solving pattern recognition problems. In *Proceedings of the International Conference on Pattern Recognition Applications and Methods - Volume 1: ICPRAM.*, pages 271–278. INSTICC, SciTePress, 2015. 5
- [2] Salvador Aguinaga, David Chiang, and Tim Weninger. Learning hyperedge replacement grammars for graph generation. *IEEE Transactions on Pattern Analysis and Machine Intelligence*, 41(3):625–638, 2019. 1, 3
- [3] James P. Bagrow and Erik M. Bollt. An information-theoretic, all-scales approach to comparing networks. *Applied Network Science*, 4(1):45, Jul 2019. 8
- [4] Mohammadhossein Bateni, Soheil Behnezhad, Mahsa Derakhshan, MohammadTaghi Hajiaghayi, Raimondas Kiveris, Silvio Lattanzi, and Vahab Mirrokni. Affinity clustering: Hierarchical clustering at scale. In I. Guyon, U. Von Luxburg, S. Bengio, H. Wallach, R. Fergus, S. Vishwanathan, and R. Garnett, editors, *Advances in Neural Information Processing Systems*, volume 30. Curran Associates, Inc., 2017. 3
- [5] Austin R. Benson, Rediet Abebe, Michael T. Schaub, Ali Jadbabaie, and Jon Kleinberg. Simplicial closure and higher-order link prediction. *Proceedings of the National Academy of Sciences*, 115(48):E11221–E11230, 2018. 1
- [6] Vincent D. Blondel, Jean-Loup Guillaume, Renaud Lambiotte, and Etienne Lefebvre. Fast unfolding of communities in large networks. *Journal of Statistical Mechanics: Theory and Experiment*, 2008(10):P10008, oct 2008. 3
- [7] Peter Bubenik. Statistical topological data analysis using persistence landscapes. *J. Mach. Learn. Res.*, 16(1):77–102, jan 2015. 3
- [8] Fan Chung and Linyuan Lu. *Complex Graphs and Networks (Cbms Regional Conference Series in Mathematics)*. American Mathematical Society, USA, 2006. 6
- [9] Stéphan Cléménçon, Hector De Arazoza, Fabrice Rossi, and Viet Chi Tran. Hierarchical clustering for graph visualization. 2012. 3
- [10] David Cohen-Steiner, Herbert Edelsbrunner, and John Harer. Stability of persistence diagrams. In *Proceedings of the Twenty-First Annual Symposium on Computational Geometry*, SCG ’05, page 263–271, New York, NY, USA, 2005. Association for Computing Machinery. 3
- [11] Sergey N. Dorogovtsev, Alexander V. Goltsev, and José F.F. Mendes. k-core organization of complex networks. *Phys Rev Lett*, 96(4):040601, February 2006. 3
- [12] Paul Erdős and Alfréd Rényi. On random graphs i. *Publicationes Mathematicae Debrecen*, 6:290, 1959. 6
- [13] Yitian Gao, Hongwei Fang, and Ke Ni. A hierarchical clustering method of hydrogen bond networks in liquid water undergoing shear flow. *Scientific Reports*, 11(1):9542, May 2021. 3

- [14] Arthur Gretton, Karsten M. Borgwardt, Malte J. Rasch, Bernhard Schölkopf, and Alexander Smola. A kernel two-sample test. *Journal of Machine Learning Research*, 13(25):723–773, 2012. 8
- [15] Minghao Guo, Veronika Thost, Beichen Li, Payel Das, Jie Chen, and Wojciech Matusik. Data-efficient graph grammar learning for molecular generation. In *International Conference on Learning Representations*, 2022. 1, 3
- [16] Aric A. Hagberg, Daniel A. Schult, and Pieter J. Swart. Exploring network structure, dynamics, and function using networkx. In Gaël Varoquaux, Travis Vaught, and Jarrod Millman, editors, *Proceedings of the 7th Python in Science Conference*, pages 11 – 15, Pasadena, CA USA, 2008. 6
- [17] Lars Hagen and Andrew B. Kahng. New spectral methods for ratio cut partitioning and clustering. *IEEE Transactions on Computer-Aided Design of Integrated Circuits and Systems*, 11(9):1074–1085, 1992. 3
- [18] Steve Hanneke, Wenjie Fu, and Eric P. Xing. Discrete temporal models of social networks. *Electronic Journal of Statistics*, 4(none):585 – 605, 2010. 1
- [19] Justus Hibshman, Satyaki Sikdar, and Tim Weninger. Towards interpretable graph modeling with vertex replacement grammars. In *2019 IEEE International Conference on Big Data (Big Data)*, pages 770–779, 2019. 3
- [20] Justus Isaiah Hibshman, Daniel Gonzalez, Satyaki Sikdar, and Tim Weninger. Joint subgraph-to-subgraph transitions: Generalizing triadic closure for powerful and interpretable graph modeling. In *Proceedings of the 14th ACM International Conference on Web Search and Data Mining, WSDM '21*, page 815–823, New York, NY, USA, 2021. Association for Computing Machinery. 1
- [21] Paul W. Holland, Kathryn Blackmond Laskey, and Samuel Leinhardt. Stochastic blockmodels: First steps. *Social Networks*, 5(2):109–137, 1983. 6
- [22] Petter Holme and Jari Saramäki. Temporal networks. *Physics Reports*, 519(3):97–125, 2012. 2
- [23] Hiroshi Kajino. Molecular hypergraph grammar with its application to molecular optimization. In Kamalika Chaudhuri and Ruslan Salakhutdinov, editors, *Proceedings of the 36th International Conference on Machine Learning*, volume 97 of *Proceedings of Machine Learning Research*, pages 3183–3191. PMLR, 09–15 Jun 2019. 1
- [24] Daniel Le Métayer. Software architecture styles as graph grammars. In *Proceedings of the 4th ACM SIGSOFT Symposium on Foundations of Software Engineering, SIGSOFT '96*, page 15–23, New York, NY, USA, 1996. Association for Computing Machinery. 1
- [25] Erhan Leblebici, Anthony Anjorin, and Andy Schürr. Inter-model consistency checking using triple graph grammars and linear optimization techniques. In Marieke Huisman and Julia Rubin, editors, *Fundamental Approaches to Software Engineering*, pages 191–207, Berlin, Heidelberg, 2017. Springer Berlin Heidelberg. 1
- [26] Renjie Liao, Yujia Li, Yang Song, Shenlong Wang, Will Hamilton, David K Duvenaud, Raquel Urtasun, and Richard Zemel. Efficient graph generation with graph recurrent attention networks. *Advances in neural information processing systems*, 32, 2019. 1
- [27] Catherine Matias and Vincent Miele. Statistical clustering of temporal networks through a dynamic stochastic block model. *Journal of the Royal Statistical Society. Series B (Statistical Methodology)*, 79(4):1119–1141, 2017. 1
- [28] Leslie O’Bray, Bastian Rieck, and Karsten Borgwardt. Filtration curves for graph representation. In *Proceedings of the 27th ACM SIGKDD Conference on Knowledge Discovery & Data Mining, KDD '21*, page 1267–1275, New York, NY, USA, 2021. Association for Computing Machinery. 3
- [29] Tiago P. Peixoto. The graph-tool python library. *figshare*, 2014. 6
- [30] Corey Pennycuff, Satyaki Sikdar, Catalina Vajiac, David Chiang, and Tim Weninger. Synchronous hyperedge replacement graph grammars. In Leen Lambers and Jens Weber, editors, *Graph Transformation*, pages 20–36, Cham, 2018. Springer International Publishing. 1
- [31] Kijung Shin, Tina Eliassi-Rad, and Christos Faloutsos. Corescope: Graph mining using k-core analysis — patterns, anomalies and algorithms. In *2016 IEEE 16th International Conference on Data Mining (ICDM)*, pages 469–478, 2016. 3
- [32] Satyaki Sikdar, Justus Hibshman, and Tim Weninger. Modeling graphs with vertex replacement grammars. In *2019 IEEE International Conference on Data Mining (ICDM)*, pages 558–567, 2019. 1, 3, 4, 6
- [33] Satyaki Sikdar, Neil Shah, and Tim Weninger. Attributed graph modeling with vertex replacement grammars. In *Proceedings of the Fifteenth ACM International Conference on Web Search and Data Mining, WSDM '22*, page 928–936, New York, NY, USA, 2022. Association for Computing Machinery. 1, 3
- [34] Joshua Southern, Jeremy Wayland, Michael Bronstein, and Bastian Rieck. Curvature filtrations for graph generative model evaluation, 2023. 3
- [35] V. A. Traag, L. Waltman, and N. J. van Eck. From louvain to leiden: guaranteeing well-connected communities. *Scientific Reports*, 9(1):5233, Mar 2019. 3
- [36] Ludo Waltman and Nees Jan van Eck. A smart local moving algorithm for large-scale modularity-based community detection. *The European Physical Journal B*, 86(11):471, Nov 2013. 3
- [37] Zhenyi Wang, Yanjie Zhong, Zhaofeng Ye, Lang Zeng, Yang Chen, Minglei Shi, Zhiyuan Yuan, Qiming Zhou, Mingping Qian, and Michael Q Zhang. MarkovHC: Markov hierarchical clustering for the topological structure of high-dimensional single-cell omics data with transition pathway and critical point detection. *Nucleic Acids Research*, 50(1):46–56, 12 2021. 3

- [38] Tim Wenginger Xinyi Wang, Salvador Aguinaga and David Chiang. Growing better graphs with latent-variable probabilistic graph grammars. In *Proceedings of the 14th International Workshop on Mining and Learning with Graphs (MLG)*, 2018. 1, 3
- [39] Chencheng Xu, Qiao Liu, Minlie Huang, and Tao Jiang. Reinforced molecular optimization with neighborhood-controlled grammars. In H. Larochelle, M. Ranzato, R. Hadsell, M.F. Balcan, and H. Lin, editors, *Advances in Neural Information Processing Systems*, volume 33, pages 8366–8377. Curran Associates, Inc., 2020. 1
- [40] Rex Ying, Jiaxuan You, Christopher Morris, Xiang Ren, William L. Hamilton, and Jure Leskovec. Hierarchical graph representation learning with differentiable pooling. In *Proceedings of the 32nd International Conference on Neural Information Processing Systems, NIPS’18*, page 4805–4815, Red Hook, NY, USA, 2018. Curran Associates Inc. 3
- [41] Jiaxuan You, Rex Ying, Xiang Ren, William Hamilton, and Jure Leskovec. Graphrnn: Generating realistic graphs with deep auto-regressive models. In *International conference on machine learning*, pages 5708–5717. PMLR, 2018. 1, 6
- [42] Shihua. Zhang, Xue-Mei Ning, and Xiang-Sun Zhang. Graph kernels, hierarchical clustering, and network community structure: experiments and comparative analysis. *The European Physical Journal B*, 57(1):67–74, May 2007. 3
- [43] Allan Zhao, Jie Xu, Mina Konaković-Luković, Josephine Hughes, Andrew Spielberg, Daniela Rus, and Wojciech Matusik. Robogrammar: Graph grammar for terrain-optimized robot design. *ACM Trans. Graph.*, 39(6), nov 2020. 1